Supplemental material

Kana et al., https://doi.org/10.1084/jem.20182037

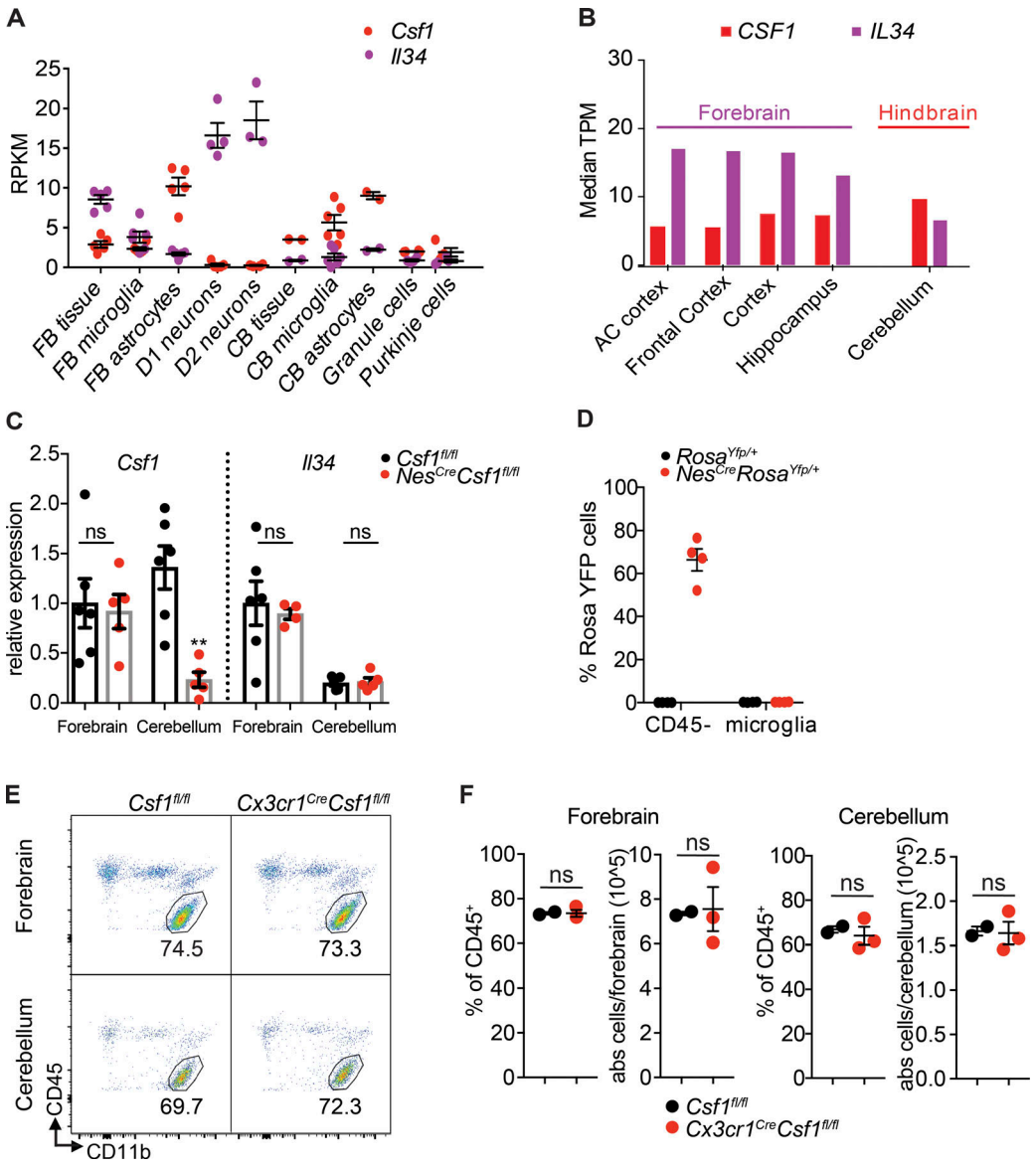

Figure S1. **Distinct expression patterns of CSF-1 and IL-34 RNA in mice and humans. (A)** Normalized (RPKM) *Csf1* and *Il34* mRNA expression levels in different brain tissues, glial cells, and neuronal cell populations from the forebrain (FB) and cerebellum (CB). Expression data generated by TRAP sequencing. *n* = 4 or 5/tissue or cell type. **(B)** Normalized (median TPM) gene expression of *IL34* and *CSF1* mRNA transcripts from different human forebrain regions and cerebellum. Expression data generated by RNA-seq and downloaded from the Human Protein Atlas database. AC, anterior cingulate. **(C)** Relative qPCR expression of *Csf1* and *Il34* mRNA in forebrain and cerebellum from 6–7-wk-old $Csf1^{fl/fl}$ and $Nes^{Cre}Csf1^{fl/fl}$ mice. All groups normalized to $Csf1^{fl/fl}$ forebrain expression. *n* = 3 or 4 mice/group. Data are a pool of two independent experiments. **(D)** Flow-cytometric analysis showing *Yfp* (Nes) expression in $DAPI^-CD45^-CX3CR1^-$ parenchymal cells and $DAPI^-CD45^{int}CX3CR1^{hi}$ microglia from adult $Rosa^{Yfp/+}$ and $Nes^{Cre}Rosa^{Yfp/+}$ brains. *n* = 3 or 4 mice/group. **(E and F)** Representative pseudocolor plots (E) and quantification (F) of flow-cytometric analysis of forebrain and cerebellar $doublet^-DAPI^-CD11b^+CD45^{int}$ microglia from $Csf1^{fl/fl}$ and $Cx3cr1^{Cre}Csf1^{fl/fl}$ mice. Numbers adjacent to gate show percentages of $CD45^+$ cells. *n* = 2 or 3 mice/group. Graphs show mean ± SEM. ns, not significant.

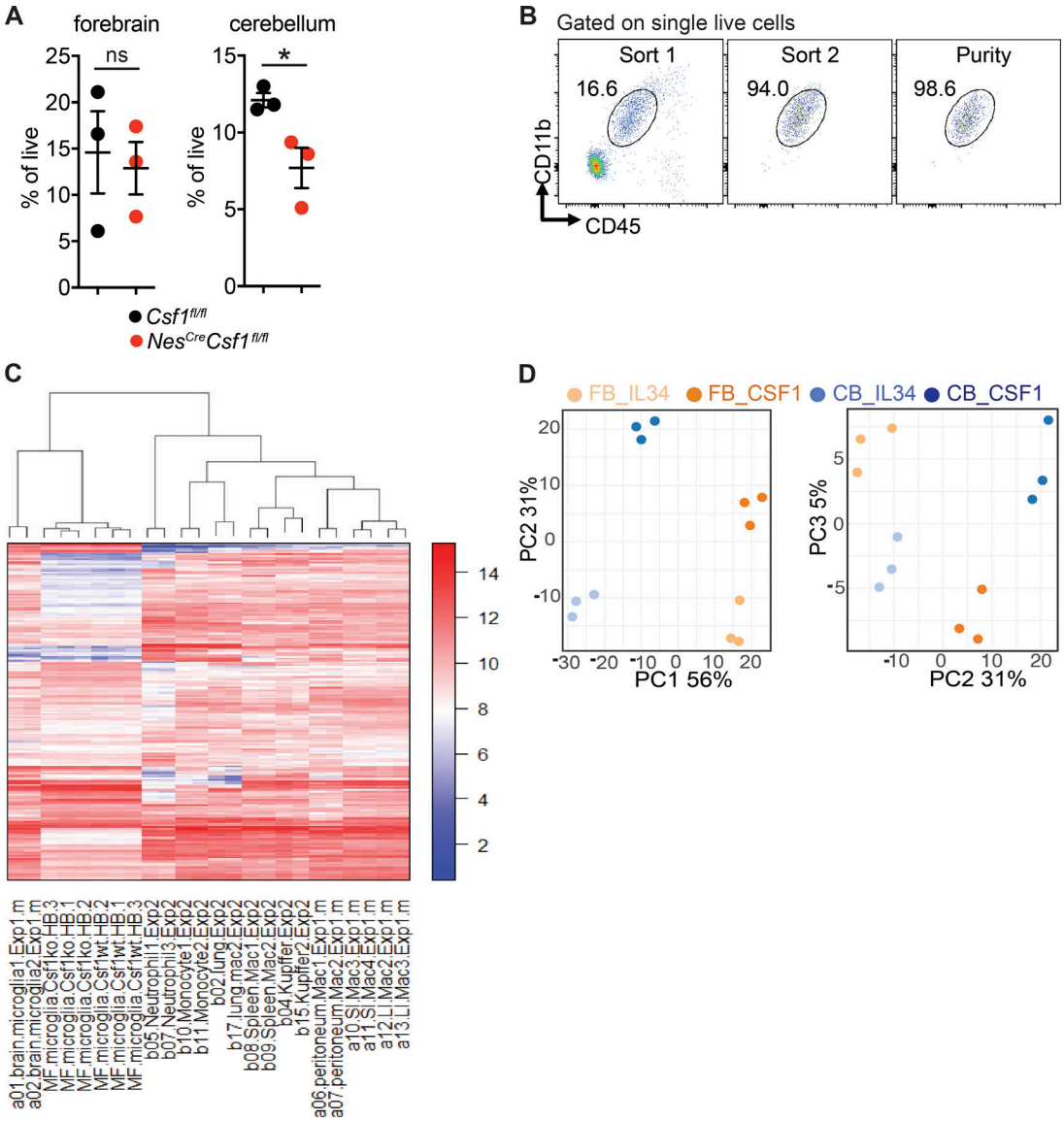

Figure S2. ***Nes^{Cre}Csf1$^{fl/fl}$* microglia profile clusters with published microglia profile and distinct clustering of CSF-1– or IL-34–stimulated forebrain and cerebellar neonatal microglia. (A)** Flow-cytometric quantification of doublet^{-}DAPI^{-}CD11b^{+}CD45^{int} microglia from P8 forebrain (left) and cerebellum (right) of *Csf1$^{fl/fl}$* and *Nes^{Cre}Csf1$^{fl/fl}$* littermates, used for NexGen sequencing. *n* = 3 mice/group. ns, not significant. **(B)** Flow cytometry sorting strategy for microglia, used for NexGen sequencing. Cells were double sorted to reach purity >98%. *n* = 3 mice/group. **(C)** Heat map of hierarchically clustered transcriptomes of P8 *Csf1$^{fl/fl}$* and *Nes^{Cre}Csf1$^{fl/fl}$* cerebellar microglia alongside previously published expression profiles of monocytes, tissue-resident macrophages, and neutrophils (Lavin et al., 2014). *Csf1$^{fl/fl}$* and *Nes^{Cre}Csf1$^{fl/fl}$* microglia cluster with the other microglial transcriptomes. Scale represents row z-score. **(D)** Principal component analysis of stimulated neonatal cortical and cerebellar microglia showing discrete clustering of samples. PC1 on the left plot shows 56% of variability in the expression data can be explained by brain region of microglia, while PC2 on the left and right plots shows 31% of variability can be explained by cytokine stimulation, regardless of brain region origin of the microglia. Graphs show means ± SEM. *, P ≤ 0.05.

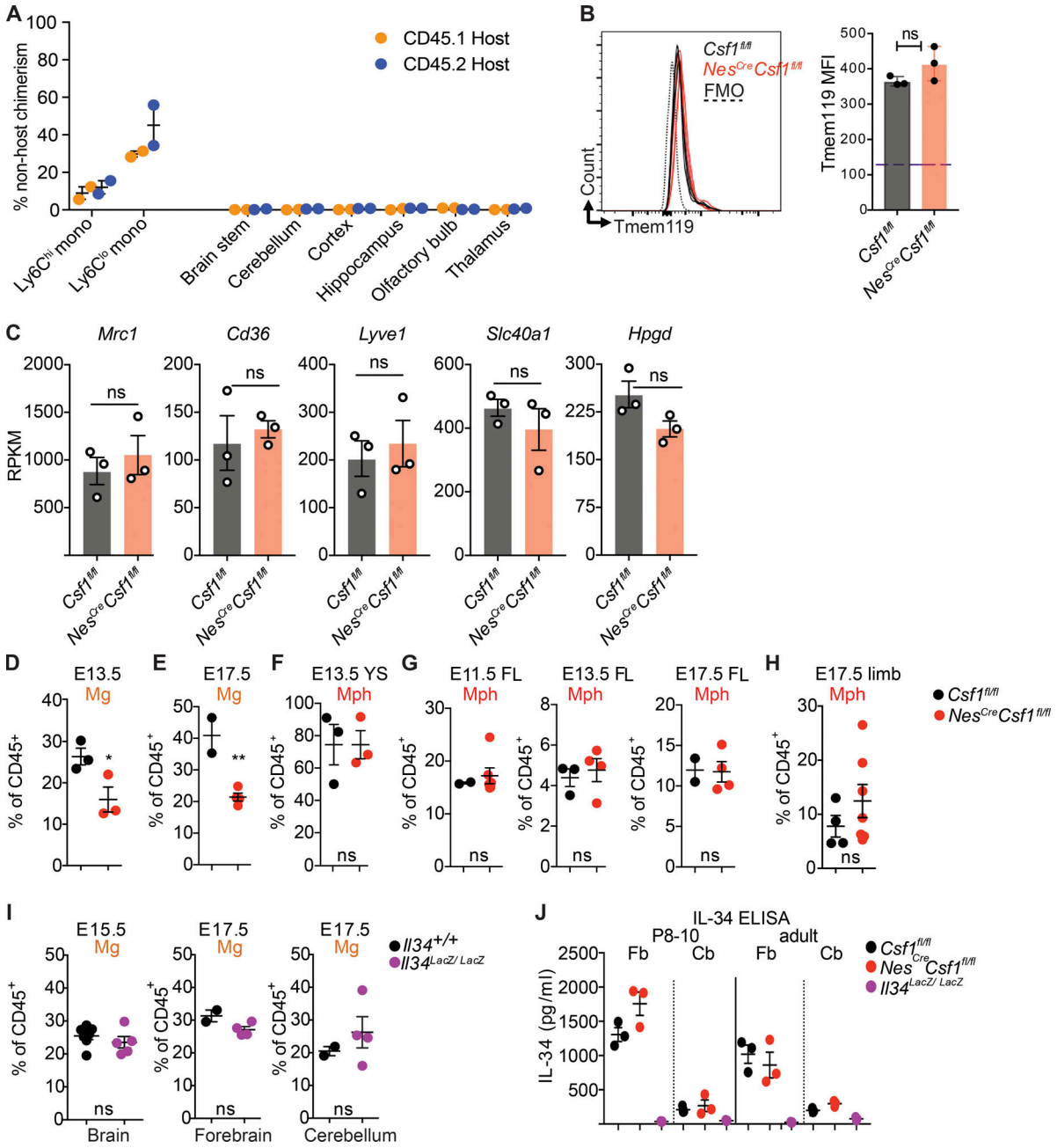

Figure S3. **Characterization of cerebellar microglia and embryonic macrophages in control and CSF-1–deficient mice. (A)** Percent chimerism of monocytes and total CD45⁺ cells in tissue of various brain regions from CD45.1 and CD45.2 parabionts anastomosed for 3 mo. *n* = 2 mice/group. **(B)** Flow-cytometric analysis of Tmem119 expression in cerebellar microglia from control and CSF-1–deficient mice including fluorescence minus one (FMO) control. *n* = 3 mice/genotype. Data are representative of two independent experiments. **(C)** Normalized (RPKM) mRNA expression of select perivascular macrophage genes in microglia from *Csf1*$^{fl/fl}$ and *Nes*^{Cre}*Csf1*$^{fl/fl}$ P8 cerebella. *n* = 3 mice/group. **(D and E)** Quantification of the percentage of microglia in whole brain rudiments from embryos at E13.5 (D) and E17.5 (E) in *Csf1*$^{fl/fl}$ and *Nes*^{Cre}*Csf1*$^{fl/fl}$ mice. *n* = 2 or 3 mice/group at each age. Data are representative from at least two independent experiments. *, P ≤ 0.05. **(F–H)** Quantification of the percentage of macrophages (Mph) in yolk sac (YS; F), fetal liver (FL; G), and limbs (H) of embryos at E13.5, E11.5, and E17.5 in *Csf1*$^{fl/fl}$ and *Nes*^{Cre}*Csf1*$^{fl/fl}$ mice. *n* = 2–7 mice/group at each age. Data are pooled from at least two independent experiments. **(I)** Quantification of the percentage of microglia (Mg) in whole brains from E15.5, and isolated forebrain and cerebellum from E17.5 *Il34*$^{wt/wt}$ and *Il34*$^{LacZ/LacZ}$ mice. *n* = 2–7 mice/group. Data are pooled from at least two independent experiments. **(J)** ELISA for IL-34 protein (pg/ml) from P8–10 and adult forebrain (Fb) and cerebellar (Cb) brain tissue from *Csf1*$^{fl/fl}$, *Nes*^{Cre}*Csf1*$^{fl/fl}$, and *Il34*$^{LacZ/LacZ}$ mice. *n* = 3 mice/group. Graphs show mean ± SEM. ns, not significant; **, P ≤ 0.01 using Student's *t* tests. MFI, mean fluorescence intensity.

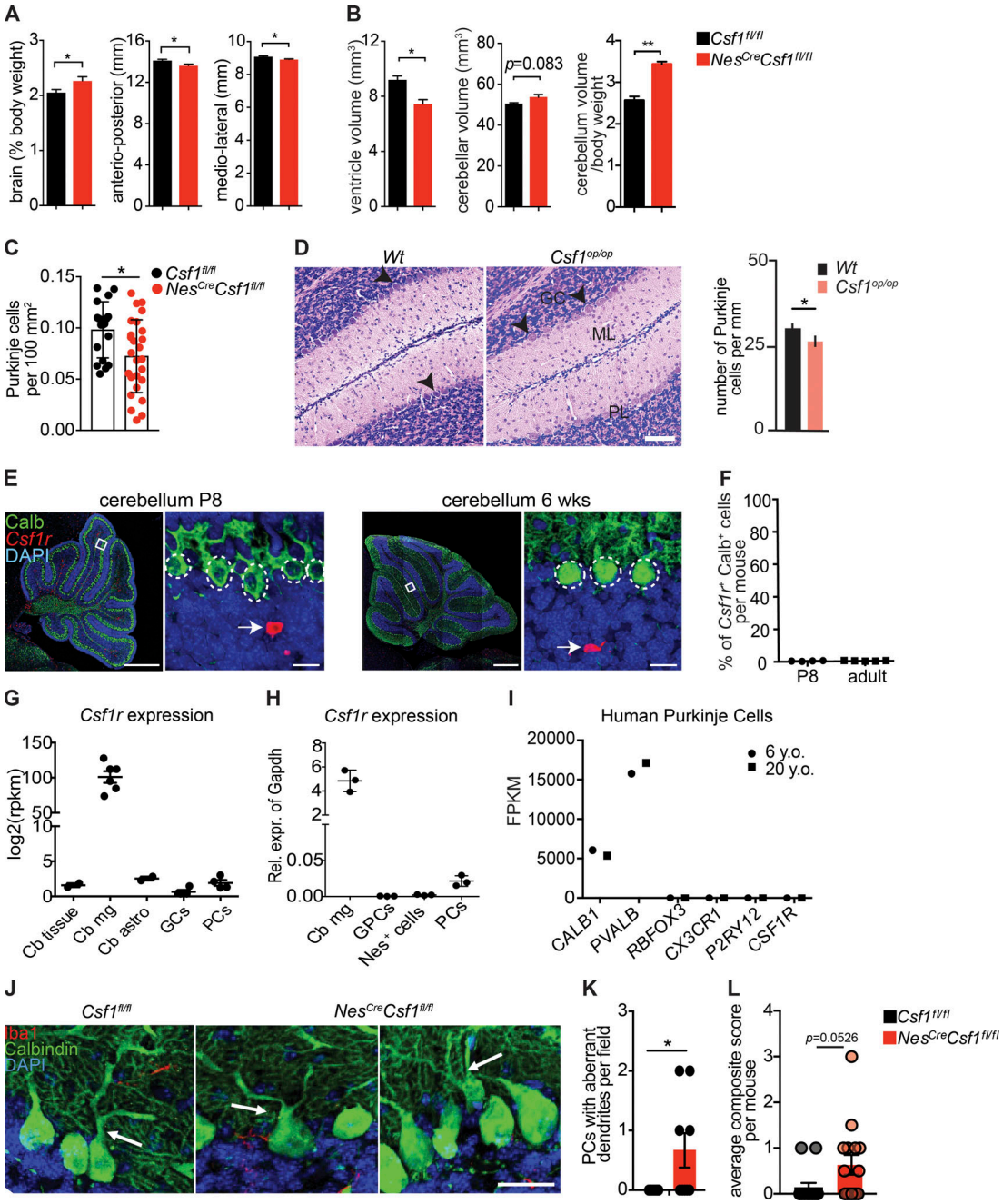

Figure S4. **Morphological and behavioral alterations in CSF-1–deficient mice. (A and B)** Quantification of brain mass and brain size (A), cerebellar ventricular volume, total cerebellar volume, and total cerebellar volume normalized to body weight (B) as measured by MRI in control and $Nes^{Cre}Csf1^{fl/fl}$ mice. *n* = 3 mice/group, one experiment. **(C)** Quantification of calb⁺ PC per mm² of PC and molecular cell layers in P21 $Csf1^{fl/fl}$ and $Nes^{Cre}Csf1^{fl/fl}$ cerebella. *n* = 4 mice/group, four to six sections/mouse. **(D)** Representative H&E stainings (left) and quantification (right) of PCs from 2-wk-old WT and $Csf1^{op/op}$ cerebella. Black arrowheads point to PCs. GC, granule cell layer; ML, molecular layer; PL, PC layer. *n* = 15 sections from three mice/genotype. Scale bar, 75 µm. Representative experiment from two independent experiments. **(E and F)** Representative immunofluorescence images (E) and quantification (F) of *Csf1r* mRNA expression in calb⁺ PCs from P8 and 6-wk-old WT cerebella. Scale bars, 500 µm (overview) and 20 µm (inserts). *n* = 4–5 mice/group. Image processing was performed using Zen 2011 software (Zeiss). Whole cerebellum images were stitched together using the "tile" function of Zen software. **(G)** Normalized (RPKM) *Csf1r* mRNA expression in different cell-types from adult WT cerebella. Expression data generated by TRAP sequencing. Cb, cerebellum; astro, astrocyte; GCs, granule cells. *n* = 2–6 mice/cell type. **(H)** Relative expression of *Csf1r* in different cell types from P6 WT cerebella. Expression data generated by RT-PCR. GPCs, granule precursor cells. *n* = 3 mice/cell type. **(I)** Normalized expression (fragments per kilobase of transcript per million mapped reads; FPKM) of neuronal and microglial specific genes in laser capture micro-dissected PCs from cerebella of a 6-yr-old and 20-yr-old patient. Expression data generated by RNA-seq and downloaded from ENCODE consortium. 6-yr-old: *n* = 30 cells, 20-yr-old: *n* = 20 cells. **(J and K)** Representative immunofluorescence stainings (J) and quantification (K) of calb⁺ PCs with multiple dendrites emerging from their soma, in adult $Csf1^{fl/fl}$ and $Nes^{Cre}Csf1^{fl/fl}$ cerebella. *n* = 3 mice/group, *n* = 7–11 high-power fields/genotype. White arrows point to PC dendrites. Scale bar, 50 µm. **(L)** Quantification of the percentage of mice positive for ataxia across multiple models (composite score of kyphosis presence, gait analysis, hanging wire test, ledge test, and hind limb clasping presence) in adult $Csf1^{fl/fl}$ and $Nes^{Cre}Csf1^{fl/fl}$ mice. *n* = 14 or 15 mice/group. Graphs show means ± SEM. *, P ≤ 0.05; **, P ≤ 0.01, using Student's *t* test.

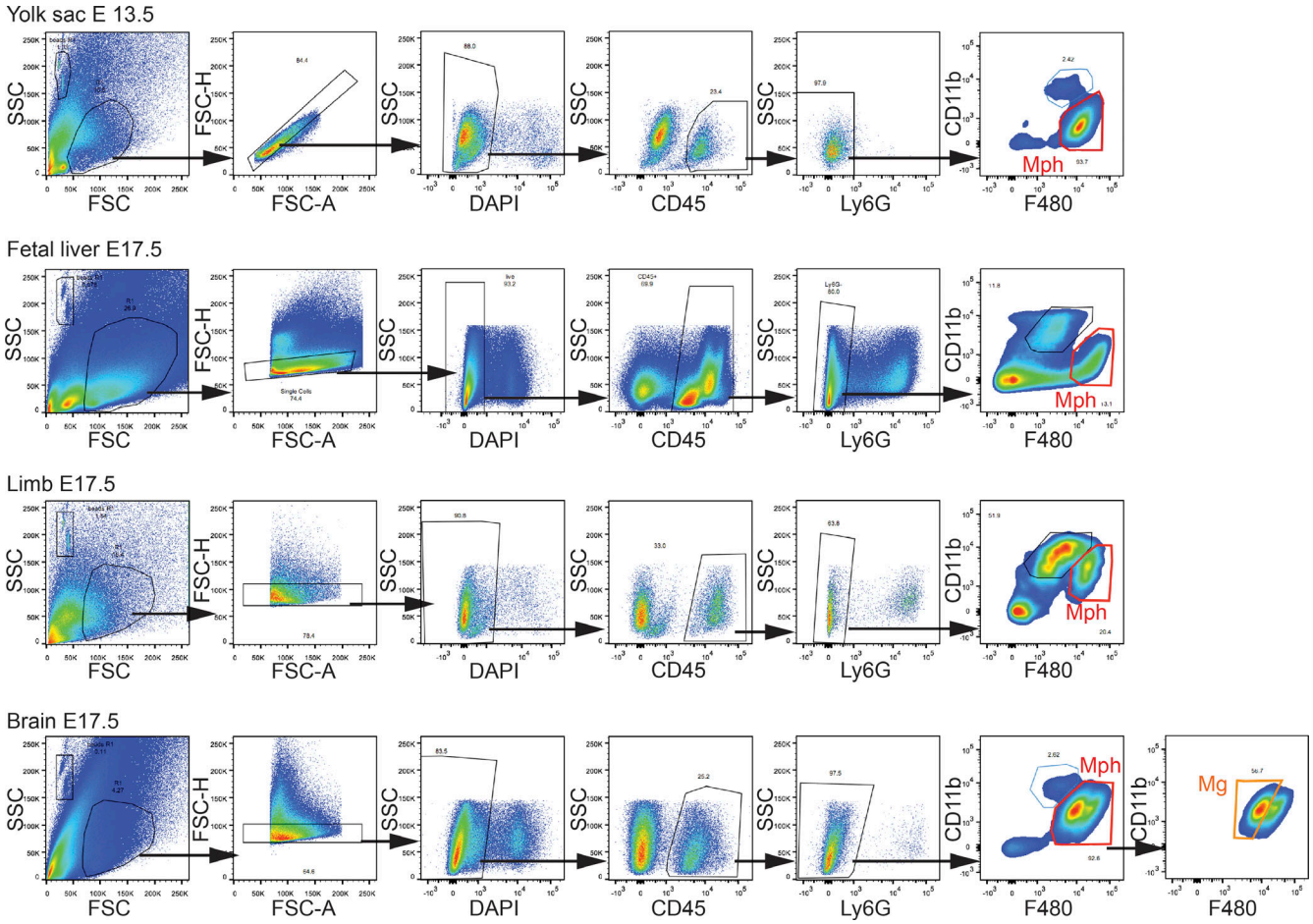

Figure S5. **Gating strategies for flow cytometry analysis of embryonic tissues in CSF-1–deficient mice.** Representative gating strategies of yolk sac, fetal liver, limbs, and brains (shown is forebrain) of *Csf1*$^{fl/fl}$ and *Nes*^{Cre}*Csf1*$^{fl/fl}$ embryos at the specified ages of development. These gating strategies were used in Fig. 3 A and Fig. S3, D–J. Mph, macrophages; Mg, microglia; SSC, side scatter; FSC, forward scatter; FSC-A, forward scatter area; FSC-H, forward scatter height.

Tables S1–S3 are provided online as a single Excel file. Table S1 shows GO term pathways for RNA-seq expression data of purified human cerebellar and forebrain microglia. Table S2 shows GO term pathways for RNA-seq expression data of sorted P8 and adult Csf1$^{fl/fl}$ and Nes^{Cre}Csf1$^{fl/fl}$, and adult Il34$^{wt/wt}$ and Il34$^{LacZ/LacZ}$ cerebellar and forebrain microglia. Table S3 shows GO term pathways for RNA-seq expression data of cultured and sorted primary neonatal cerebellar and forebrain microglia stimulated with CSF-1 or IL-34.

Reference

Lavin, Y., D. Winter, R. Blecher-Gonen, E. David, H. Keren-Shaul, M. Merad, S. Jung, and I. Amit. 2014. Tissue-resident macrophage enhancer landscapes are shaped by the local microenvironment. *Cell.* 159:1312–1326. https://doi.org/10.1016/j.cell.2014.11.018